Environmental Pollution 286 (2021) 117227

Contents lists available at ScienceDirect

Environmental Pollution

journal homepage: www.elsevier.com/locate/envpol

# Conductive property of secondary minerals triggered Cr(VI) bioreduction by dissimilatory iron reducing bacteria

Ke Zhang [a], Na Li [a], Peng Liao [b], Yuwen Jin [a], Qiongyao Li [a], Min Gan [a], Yaozong Chen [a], Peng He [a], Fang Chen [a], Mingxian Peng [a], Jianyu Zhu [a, *]

[a] School of Minerals Processing and Bioengineering, Key Laboratory of Biohydrometallurgy of Ministry of Education, Central South University, Changsha, 410083, China
[b] State Key Laboratory of Environmental Geochemistry, Institute of Geochemistry, Chinese Academy of Sciences, 99 Lingcheng West Road, Guiyang, 550081, China

ARTICLE INFO

*Article history:*
Received 15 January 2021
Received in revised form
10 April 2021
Accepted 21 April 2021
Available online 24 April 2021

*Keywords:*
Semiconductor secondary minerals
Cr(VI) reduction
Adsorption Fe(III)/Fe(II) cycling
Direct electron transfer

ABSTRACT

Although secondary minerals have great potential for heavy metal removal, their impact on chromium biogeochemistry in subsurface environments associated with dissimilatory iron reducing bacteria (DIRB) remains poorly characterized. Here, we have investigated the mechanisms of biogenic secondary minerals on the rate of Cr(VI) bioreduction with *shewanella oneidensis* MR-1. Batch results showed that the biogenic secondary minerals, schwertmannite and jarosite, appreciably increased the Cr(VI) bioreduction rate. UV–vis diffuse reflection spectra showed that schwertmannite and jarosite are semiconductive minerals, which can be activated by MR-1, followed by transferred conduction electrons toward Cr(VI). Cyclic voltammetry and Tafel analysis suggested that the resistance of secondary minerals is a dominant factor controlling Cr(VI) bioreduction. In addition, Cr(VI) adsorption on secondary minerals through ligand exchange promoted Cr(VI) bioreduction by decreasing the electron transfer distance between MR-1 and chromate. Fe(III)/Fe(II) cycling in schwertmannite and jarosite also contributed to Cr(VI) bioreduction as reflected by X-ray photoelectron spectroscopy and Fourier transform infrared spectrometer. Complementary characterizations further verified the contributions of Fe(III)/Fe(II) cycling, Cr(VI) adsorption, and conduction band electron transfer to enhanced Cr(VI) bioreduction. This study provides new insights on the understanding of Cr(VI) bioreduction by semiconductor minerals containing sulfate in subsurface environments.



## 1. Introduction

Subsurface contamination by hexavalent chromium (Cr(VI)) has posed severe risks to aquifer and public health worldwide (Agrawal et al., 2006; Costa and Klein, 2006). Cr(VI) can penetrate the cell membrane through the sulfate transport system because chromate has a similar structure to sulfate (Holland and Avery, 2011). In the cell, Cr(VI) is reduced to Cr(III) by both enzymatic and nonenzymatic reactions producing reactive oxygen species (ROS) that can damage the cell by interacting with protein and nucleic acid (Rager et al., 2019; Zhanna et al., 2011). Cr(VI) is soluble and can be readily transported in a porous media in the subsurface environment (James et al., 1994), while Cr(III) is relatively stable and less toxic. Therefore, the conversion of Cr(VI) to Cr(III) is an efficient strategy for the remediation of Cr(VI) in groundwater(Jiang et al., 2019).

Microbial reduction is a safe and effective method to transform Cr(VI) into Cr(III). DIRB, whose respiratory versatility, has prompted interest in its use in bioremediation, which can reduce a variety of toxic metal decontaminations, including iron (III) (Fu et al., 2016), vanadium(V) (Wang et al., 2017), uranium(VI) (Sheng and Fein, 2014), technetium(VII) (Marshall et al., 2008), Cr(VI)(Gong et al., 2018). Significant, DIRB directly reduces Cr(VI) through the extracellular electron transfer (EET) pathway (Cheng et al., 2020) , but the efficiency of electron transfer between DIRB and Cr(VI) is a rate limiting step in the Cr(VI) bioreduction. Redox mediators that can be reversibly oxidized and reduced like catalysts are applied as electron transfer stations to promote the electron transfer(Shi et al., 2016; Zhi et al., 2012). Among them, the most impressive is the Fe(II)/Fe(III) redox couple with the extensive reduction potential which was found to be responsible for the EET pathway of DIRB.

* Corresponding author.
*E-mail address:* zhujy@csu.edu.cn (J. Zhu).

https://doi.org/10.1016/j.envpol.2021.117227
0269-7491/

Iron bearing minerals, a major supplier of iron, can act as electron transfer stations through Fe(II)/Fe(III) to enhance the rate of EET of DIRB(Qiu et al., 2020).

In addition, iron bearing minerals can also act as electron conduits because of their electrical conductivity(Qiu et al., 2020). As a general rule, minerals can be classified into conductor minerals (Eg < 0.1 eV), semiconductor minerals (0.1 eV < Eg < 4 eV), and insulating minerals (Eg > 4 eV) based on the electronic structure of minerals (band gap). Most metal sulfide and oxide minerals are semiconductor minerals, that participate in geochemical projection and affect the electron transfer of microorganisms(Lu et al., 2019a). For example, rutile and sphalerite can produce photoelectrons under the excitation of light, which can promote the growth of *A. ferrooxidans* (Lu et al., 2012). Qiu et al. (2020) demonstrated that the iron oxide nanoparticles with higher crystallinity, such as magnetite and hematite can be utilized as conduits by bacteria to directly transfer electrons while the low-crystallinity goethite and ferrihydrite cannot. Limited studies have reported the role of natural secondary mineral as electrically conduits to mediate distant extracellular electron transfer (EET) between DIRB and Cr(VI)(Qiu et al., 2020).

Secondary minerals are transformed from primary minerals by weathering, hydrolysis, oxidation and biological action. Among them, schwertmannite ($Fe_8O_8(OH)_6(SO_4)$) and jarosite ($KFe_3(SO_4)_2(OH)_6$) have aroused great concern due to their advantages of simple synthetic processes, low cost and important roles in the sequstration of heavy metals. Schwertmannite has a good adsorption capacity for heavy metals such as Cr(VI) and As(V) via porosity and exchange reaction with the sulfate groups present in schwertmannite(Dou et al., 2013; Gan et al., 2015). Moreover, jarosite preferentially incorporates heavy metal ions into the structure to adsorb heavy metal ions such as Cr(VI) and Tl(I)(Aguilar-Carrillo et al., 2020). In nature, schwertmannite and jarosite associated with or without metals may flow into the downstream water environment, or penetrate into groundwater by gradually being buried deeply where it teemed with the DIRB. In the DIRB-secondary mineral-metals system, the biological properties of different heavy metals-loaded secondary minerals and the migration and transformation of heavy metals mediated by DIRB are different. For example, there is no dissolution of Cr(VI) and the formation of secondary phases is retarded by the reduction of DIRB on Cr(VI)-loaded schwertmannite, due to the increased microbial stability of schwertmannite once combined with Cr(VI) (Regenspurg and Peiffer, 2005; Wan et al., 2018). Compared to schwertmannite, the microbial stability of jarosite has not change in the process of combining with other heavy metals. For example, structural Fe(III) and heavy metal ions will be dissolved and the new secondary phases will be generated when Pb/As-loaded jarosite is reduced by DIRB. Although the interaction mechanism between DIRB and secondary minerals loaded with heavy metals has been explored, the role of secondary minerals on the Cr(VI) bioreduction is still lacking from the perspective of iron minerals as electron acceptors and semiconductor minerals as electron shuttle carriers.

Previous studies report that many crystalline minerals reduced by iron reducing bacteria result in a lower rate of Fe(II) generation per mole of available Fe(III) oxide than their amorphous counterparts. As such, we hypothesis that the crystallinity of secondary minerals can affect the interaction between DIRB and secondary minerals. Two types of secondary minerals (schwertmannite and jarosite) which represent different crystallization of secondary minerals were chosen to study the effect on the reduction of Cr(VI) by *Shewanella oneidensis* MR-1 (a model strain of DIRB). The findings of this study are valuable for understanding the role of secondary minerals in Cr(VI) bioreduction and are helpful to promote the application of secondary minerals in chromium pollution treatment.

## 2. Materials and methods

### 2.1. Chemicals

All reagents used in this experiment were of analytical grade or higher. The water used in the experiments was doubly deionized water ((DIW, ≥18.2 MΩ cm, Milli-Q, Millipore). All media formulations required for the experiment can be found in the supporting information.

### 2.2. Cultivation of S. oneidensis MR-1 and synthesis of minerals

*S. oneidensis* cell suspensions were prepared in 100 mL of LB medium at 30 °C for 14 h in a shaker at a speed of 200 rpm. Cells were harvested by centrifugation (3000 rpm, 30 min, 4 °C), and washed twice using sterilized bicarbonate buffer.

Schwertmannite and jarosite were prepared with biological methods by acidophilic bacteria in the laboratory. Briefly, centrifugation was used to extract *Acidithiobacillus ferrooxidans* which grew to logarithmic phase in 9 K medium. Then, the cells were added to 200 mL of pure water at pH 2 adjusted with $H_2SO_4$ or 9 K medium containing 30 g $FeSO_4 \cdot 7H_2O$ (pH 2) to synthesize schwertmannite and jarosite. *A. ferrooxidans* have the ability to oxidize and template instead of multiplying in the synthesis process. The precipitates were collected by filtration on the 7th day of synthesis, washed with acidic water (pH 2) for 3 times, and dried in vacuum drying oven. Hematite was synthesized by hydrothermal method instead of using natural minerals to avoid the interference of impurities in natural minerals. 4.052g $FeCl_3 \cdot 6H_2O$ was slowly added to 100 mL DI water, and the pH value of the solution was adjusted to 11 with 2 M KOH. The solution was then loaded to a water bath and stirred with magnetic force for 3 h. After centrifugation, the precipitates were washed three times with DI water and anhydrous ethanol respectively. After drying in an oven at 80 °C, the precipitates were calcined for 4 h at 800 °C.

### 2.3. Batch experiment

Ninety-seven millilitres of DM medium and trace elements were added into a 250 mL serum bottle to be sterilized with an autoclave. Then, nitrogen was introduced into the anaerobic operation box for 20 min to remove oxygen.

To quantify the role of schwertmannite or jarosite on Cr(VI) bioreduction, a series of identification assays was prepared by mixing: (i) MR-1 with final concentration of $4 \times 10^8$ cell/mL as a biological control system, (ii) 0.1 g schwertmannite or jarosite as a chemical control and (iii) containing both MR-1 and schwertmannite or jarosite in the culture medium. Simultaneously, the same system without adding other substances as a control was established to ensure the accuracy of Cr (VI) detection. All culture medium received 20 mM lactate as an electron donor and 3 mL Cr(VI) stock solution at a concentration of 1000 mg/L. All experiments were performed in an anoxic gloveboxe, and all experiments were carried out in a shaker at 30 °C and 200 rpm.

To assess the functionality of structural iron in minerals, hematite was used in the experiments. The experimental conditions are the same as schwertmannite systems, with the exception of replacing schwertmannite with hematite.

To verify the effect of humic acid on MR-1 + minerals + Cr(VI), the experimental conditions were the same as those of the mineral system, except that 10 mg/L of humic acid were added to each system. The jarosite system is selected to explore the influence of humic acid concentration on the MR-1 + minerals + Cr(VI). The

concentrations of humic acid were 10 mg/L, 30 mg/L and 50 mg/L.

Three replicas of each system were carried out. All media formulations required for the experiment can be found in the supporting information.

### 2.4. Characterization

Sample solutions were filtered by using 0.22 μm sterile syringe filters before analysis. Immediately after that, 1 mL of the filtered solution was analysed for aqueous Fe(II) using the 1,10-phenanthroline method (Ding et al., 2018). Briefly, the Fe(II) concentration was analyzed by adding the chelating agent 1,10-phenanthroline and then measuring the absorbance of the Fe(II)-(1,10-phenanthroline)$^{2+}_3$ complex by spectrophotometry at 510 nm. Fe(III) was quantified after reduction in the presence of hydroxylamine hydrochloride. The Cr(VI) concentrations in the filtrates were analyzed by spectrophotometry at 540 nm following the 1,5-diphenyl-carbazide method (Gan et al., 2018).

The mineral morphologies were investigated by employing JSM-6360LV scanning electron microscope coupled with energy dispersive spectrometry (SEM-EDS) (JEOL Ltd., Tokyo, Japan). X-ray diffractometer (XRD) (RINT2000, Japan) was applied to explore the mineral crystal structure, and X-ray photoelectron spectroscopy (XPS) (Thermo Fisher ESCALAB 250Xi) and Fourier Transform Infrared Spectrometer (FTIR) (Nicolet Nexus670) were used to analysis the elemental composition, valence states and functional groups of minerals. UV−vis diffuse reflection spectra (UV 2600, Shimadzu, Japan) were used to study the band gap of secondary minerals. All samples were air-dried anaerobically in a glovebox before analysis.

### 2.5. Electrochemical measurements

Electrochemical analysis was conducted to determine the effect of secondary minerals on electron transfer in MR-1+secondary mineral+Cr(VI) systems. The electrochemical measurements were performed on a CHI600E electrochemical workstation (Shanghai, China), coupled with a microcomputer. In this study, three-electrode electrochemical cell was used, including (i) a working electrode (glassy carbon electrode of 5.0 mm diameter), (ii) a reference electrode (calomel electrode) and (iii) a platinum counter electrode. The working electrode was fabricated by a slurry coating technique. The slurry consisted of mixing mineral samples (5 mg), anhydrous ethanol (400 μL), and 5% Nafion solution (100 μL). Subsequently, 6 μL of the suspended slurry was dropped onto the polished glassy carbon electrode and then dried with an infrared lamp for use in subsequent electrochemical experiments (Yang et al., 2020). Additionally, the cyclic voltammetry studies were performed with a scan rate of 0.02 V/s for both negative and positive scans. The negative scan was started from the open circuit potential (OCP) to −800 mV, then reversed to 800 mV, and finally returned to OCP. At this potential, the impedance spectra were obtained, applying an AC potential amplitude of 5 mV in the frequency range of 0.01~105 Hz. The scan of the Tafel studies started from OCP+0.25V and ended at OCP-0.25V.

## 3. Results and discussion

### 3.1. Cr(VI) removal by S. oneidensis MR-1 and secondary minerals

*S. oneidensis* MR-1 can oxidize organic compounds as electron donors and transport respiratory electrons to the outer membrane to reduce insoluble electron acceptors such as secondary minerals and Cr(VI) (Han et al., 2016). In this study, lactate was the unique electron donor of MR-1. Similar lactate consumption was observed in the MR-1/Cr(VI), MR-1+sch+Cr(VI), and MR-1+jar+Cr(VI) (Fig. 1A). In a single electron donor system, MR-1 produced electrons through intracellular metabolism of lactate, and is then transferred to extracellular via intracellular electron transfer pathways such as Mtr pathway (Han et al., 2017; Liu et al., 2017; Melton et al., 2014). Therefore, we speculated that the number of electrons from MR-1 was almost the same in the three systems. However, the Cr(VI) removal amounts for MR-1+sch+Cr(VI) (10 mg/L) and MR-1+jar+Cr(VI) (14.27 mg/L) were higher than that in the MR-1/Cr(VI) system (7.11 mg/L), but almost no removal of Cr(VI) was found in the sch/Cr(VI) system or jar/Cr(VI) system (Fig. 1B). This result implies that secondary minerals could effectively improve Cr(VI) bioreduction.

### 3.2. Effect of adsorption on Cr(VI) bioreduction

Schwertmannite has been proven to be a good adsorption material for Cr(VI) (Zhang et al., 2019). Meanwhile, it has been reported that adsorption materials enhance the removal of pollutants by shortening the distance between microorganisms and pollution (Zhao et al., 2020). Although no obvious removal of Cr(VI) was observed in the mineral/Cr(VI) system, 0.31% and 0.43% of chromium was detected on the surface of schwertmannite and jarosite, respectively (Fig. 2A). This result indicates that both schwertmannite and jarosite can adsorbs Cr(VI) to a certain degree, but the low content of minerals (1 g/L) in the experimental system limits the adsorption capacity. Meanwhile, the proportion of sulfur on schwertmannite or jarosite decreased by 88.7% (from 5.84% to 0.66%) and 45.7% (from 8.91% to 4.84%) in the minerals/Cr(VI) system, respectively, compared with the original schwertmannite and jarosite (Fig. 2A). It has been reported that schwertmannite adsorbs with Cr(VI) through the ligand exchange of sulfate radical(Gan et al., 2015). As expected, the XPS analysis shows that the sulfur-containing species of schwertmannite and jarosite are $SO_4^{2-}$ (Fig. S1). Meanwhile, compared with the original schwertmannite and jarosite, a significant downward peak intensity of 980 $cm^{-1}$ ($SO_4^{2-}$) in the sch/Cr(VI) system and of 1190, 1085 and 996 $cm^{-1}$ ($SO_4^{2-}$) in the jar/Cr(VI) system is shown in Fig. 2(B,C). These results indicate that Cr(VI) can be adsorbed to schwertmannite and jarosite by the exchange of $CrO_4^{2-}$ with the $SO_4^{2-}$ ligand consistent with previous studies(Gan et al., 2015).

To determine whether the adsorption of secondary minerals affects Cr(VI) bioreduction, the schwertmannite and jarosite under the activity of MR-1 were analysed. The XPS analysis shows that comparing with the sulfur content in jar/Cr(VI) system(4.84%), the data of that on the jarosite in jar+MR-1+Cr(VI) (3.35%) decreased 30.8%. Meanwhile, the chromium content on jar in jar+MR-1+Cr(VI) increased 4.44 times (from 0.43% to 2.34%) compared with that in the jar/Cr(VI) system. In contrast, the sulfur content on the schwertmannite in the sch+MR-1+Cr(VI) is almost the same as that in the sch/Cr(VI) system, and the chromium content on schwertmannite in the sch+MR-1+Cr(VI) increased only 1.55 times (from 0.31% to 0.79%) higher than in the sch/Cr(VI) system (Fig. 2A). The results show a negative correlation between sulfur content and chromium content in secondary minerals under the action of MR-1. This phenomenon indicates that MR-1 promotes the replacement of chromate by sulfate radicals on the surface of secondary minerals, and the promotion effect of MR-1 on jarosite is significantly better than that of schwertmannite. In addition, the zeta potential of original schwertmannite, original jarosite show that the zeta potential of jarosite is positive and higher than that of schwertmannite in neutral environment (Fig. S5, Table S2). It is reported that zeta potential of S. oneidensis MR-1 (pH 7) is -6.48 mV (Mohamed et al., 2020) , thus, more MR-1 is adsorbed on jarosite surface than on schwertmannite under neutral condition, resulting

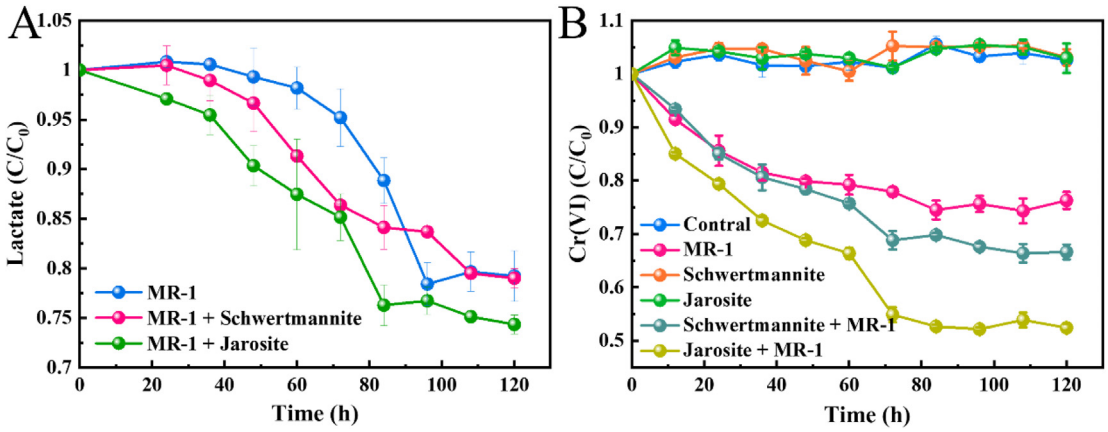


**Fig. 1.** Lactate consumption (A) and Cr(VI) reduction (B) in different experimental systems.

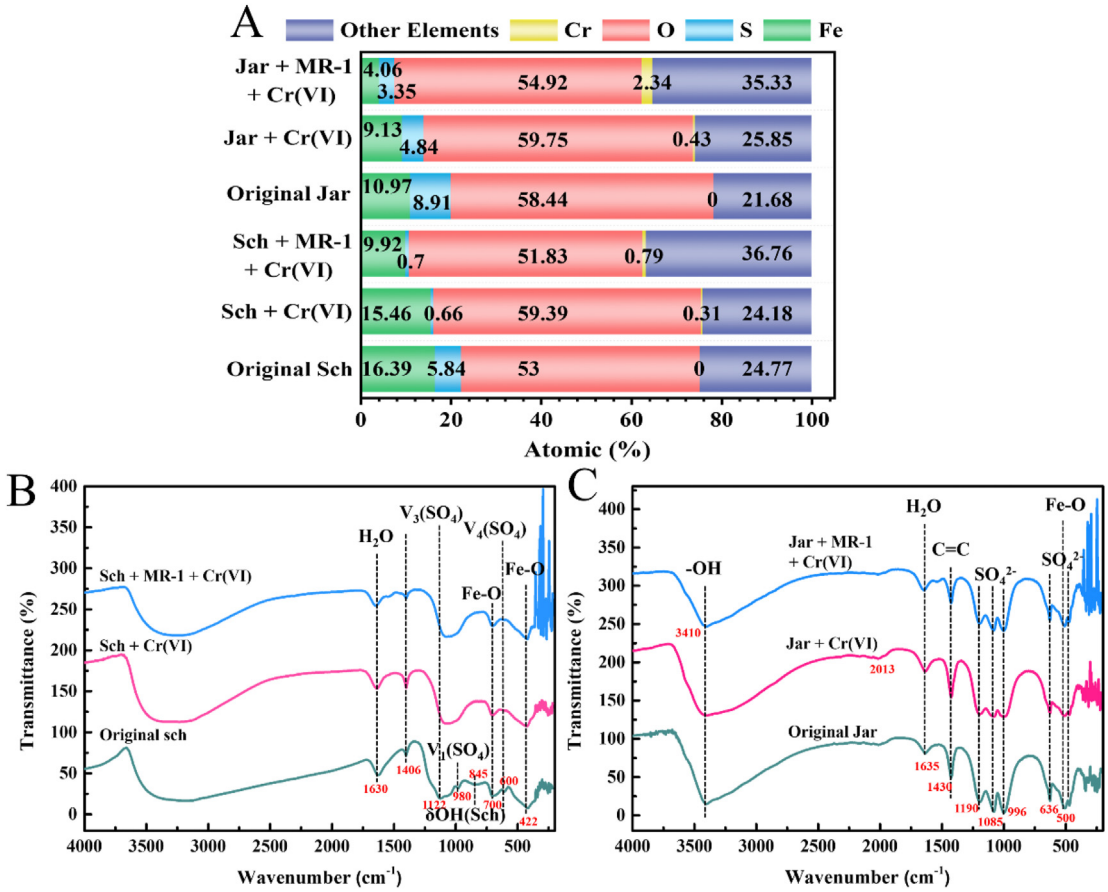


**Fig. 2.** Relative contents of elements in schwertmannite and jarosite based on XPS analysis data (A); FTIR spectrum of schwertmannite (B) and jarosite (C).

in the potential interaction between MR-1 and jarosite may be closer than that of schwertmannite. SEM imaging shows that schwertmannite possesses a pompon-like structure, and the structure of schwertmannite becomes agglomerated in sch+MR-1+Cr(VI) (Fig. S3). Thus, the sulfate sites of schwertmannite may gradually be covered up, which weakens the adsorption of Cr(VI) through the exchange of sulfate ligands. However, the structure of jarosite shrank under the action of MR-1, but the particle size decreased (Fig. S3). We deduced that jarosite may expose fresh surfaces under the stimulation of MR-1 and then expose new sulfate sites to promote the adsorption of Cr(VI). Meanwhile, we deduced that secondary minerals might directly accept the electron transfer by MR-1 based on SEM analysis of the change in mineral phase. Therefore, the adsorption of secondary minerals shortens the direct electron transfer distance between MR-1 and Cr(VI) and promote Cr(VI) bioreduction.

Additionally, the XPS analysis shows that the ratio of Cr(III)/Cr(VI) on the surface of jarosite (2.245) is significantly higher than that on the surface of schwertmannite (0.664) in MR-1+mineral+Cr(VI) (Fig. 3). Based on the adsorption content of Cr

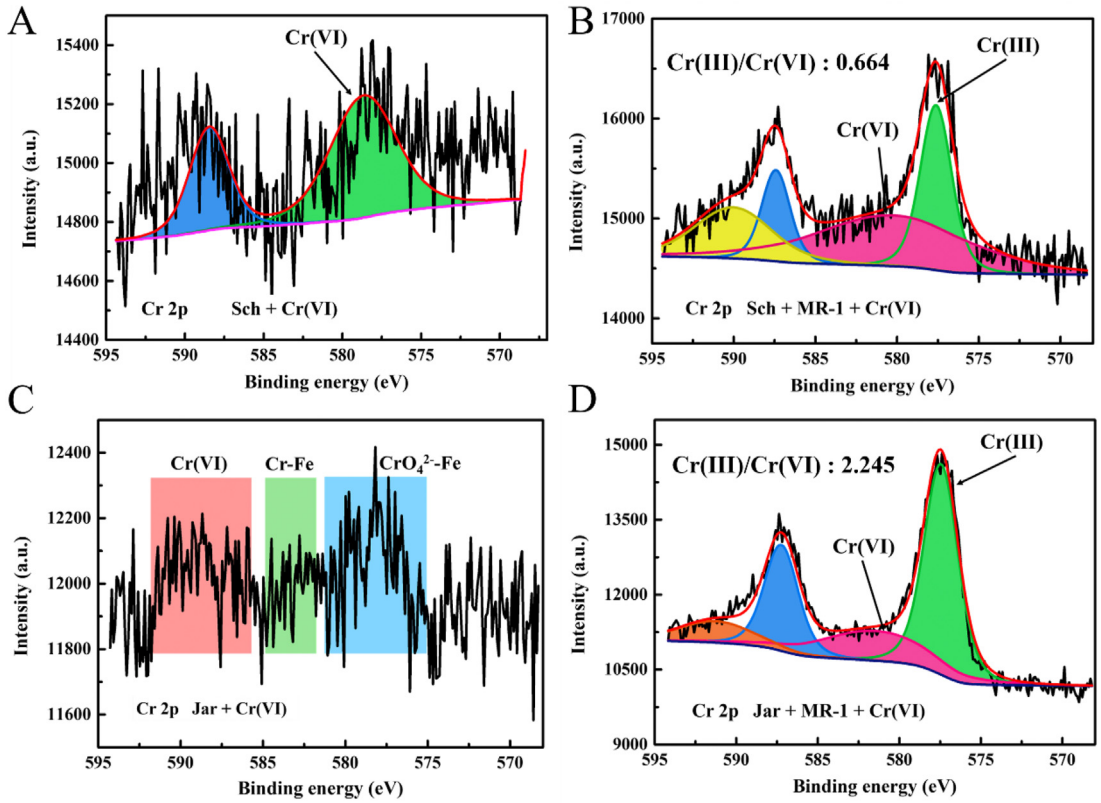


**Fig. 3.** XPS patterns of Cr in schwertmannite (A, B) and jarosite (C, D).

on the surface of the minerals, the reduced Cr(III) content on the jarosite surface is 10 times that of schwertmannite. Compared with schwertmannite, more Cr(VI) on the surface of jarosite is reduced, indicating that Cr(VI) on the surface of jarosite receives more electrons. Meanwhile, the number of electrons transferred by MR-1 to the extracellular space may be basically the same because of the same consumption of lactate in the schwertmannite and jarosite systems. Thus, we inferred that jarosite possessed a stronger ability to receive and transfer electrons than schwertmannite.

### *3.3. The electron transport pathway mediated by secondary minerals on Cr(VI) bioreduction*

The common mechanism of electron transfer mediated by iron bearing minerals is through indirect Fe(III)/Fe(II) cycling(Byrne et al., 2015) and direct conduction band electrons (Kato et al., 2012). To analyze the Fe(III)/Fe(II) cycling of secondary minerals on Cr(VI) bioreduction, $Fe^{2+}$ and total Fe concentrations in the MR-1/sch system and MR-1/jar system with or without Cr(VI) were measured. As shown in Fig. 4 (A, B), without Cr(VI), more $Fe^{2+}$ and $Fe^{T}$ was formed on the MR-1/sch system than MR-1/jar system during the reaction. Almost no $Fe^{2+}$ was detected on MR-1/sch system and MR-1/jar system when Cr(VI) was present, and a small amount of total iron was detected on MR-1/sch system and MR-1/jar system. This phenomenon is probably attributed to the biogenic $Fe^{2+}$ from MR-1 reducing Fe(III) on secondary minerals reacting with Cr(VI) to form Fe—Cr precipitates (Li et al., 2020). The production of biogenic $Fe^{2+}$ on the MR-1/sch system was higher than that of the MR-1/jar system, which may be because sch has a higher specific surface area according to the SEM results (Fig. S3). In addition, XPS data show that the content of $Fe^{2+}$ on the surface of sch is higher than that of jarosite in the absence of Cr(VI) (Fig. 4 C, D). However, no $Fe^{2+}$ was detected on the secondary mineral surface of the system containing Cr(VI) (Fig. S2). The result further confirmed that secondary minerals can promote the treatment of Cr(VI) by MR-1 through Fe(III)/Fe(II) cycling, and that Fe(III)/Fe(II) cycling in the MR-1/sch system is higher than that on MR-1/jar system. This may indicate that more Fe(III)/Fe(II) cycling on the amorphous secondary minerals system was formed to promote Cr(VI) bioreduction than on the crystalline secondary mineral system.

To determine whether the secondary minerals have semiconductor properties that produce conduction band electrons and transfer electrons when stimulated by external energy (Lu et al., 2019b), schwertmannite and jarosite were detected by ultraviolet—visible diffuse reflectance spectroscopy (Fig. 6A). According to the steep absorption edge in the detection spectrum, the band widths of schwertmannite and jarosite are 2.3 and 2.346 eV, respectively, belonging to the semiconductor range. Previous studies show that MR-1 can stimulate semiconductor minerals such as hematite to produce semiconductor electrons and transfer the electrons produced by MR-1 (Meitl et al., 2009). Therefore, we may deduce that schwertmannite and jarosite could also be excited by MR-1 to produce conduction band electrons and transfer electrons.

Mineral resistance is a major factor affecting electron transfer efficiency. Therefore, the electrical activity and resistance properties of schwertmannite and jarosite were further investigated by electrochemical detection. Cyclic voltammetry showed that the cathodic current density of the original jarosite is higher than that of schwertmannite, indicating that jarosite has better redox activity than schwertmannite (Fig. 5B). Tafel plots for the two minerals show that schwertmannite has similar ecorr to jarosite (Fig. 5C), but the polarization resistance and icorr calculated from the Tafel plots are quite different (Table S1). Compared with the original jarosite, the original schwertmannite has larger polarization resistance and

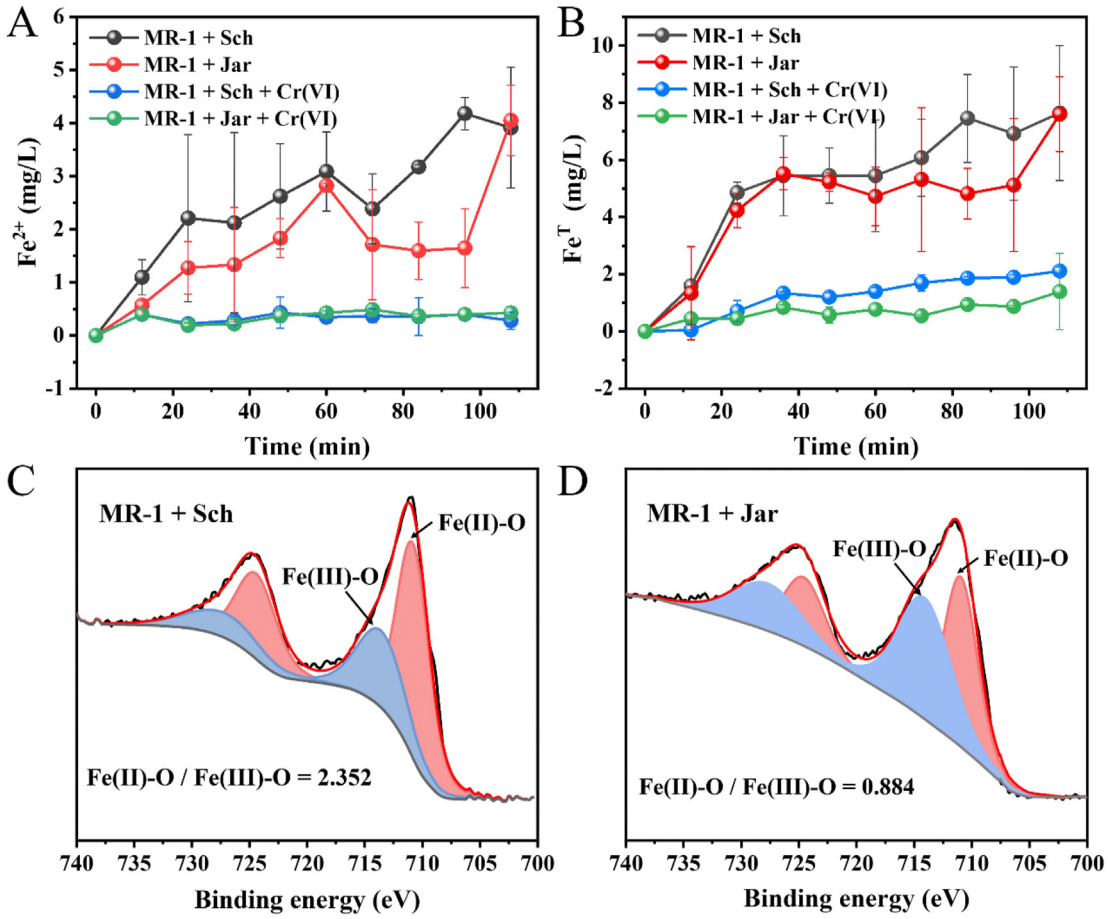


**Fig. 4.** The production of Fe(Total) (A) and $Fe^{2+}$ (B) in different system, XPS patterns of Fe in MR-1/sch system (C) and MR-1/jar (D).

smaller icorr, indicating that the conductivity of jarosite is better than that of schwertmannite. According to Fig. 1, the K value in MR-1+jar+Cr(VI) (0.0072 $h^{-1}$) is higher than that in MR-1+sch+Cr(VI) (0.0044 $^{-1}$) in the initial stage of the reaction (Fig. 5D). The reason may be that the conductivity of jarosite is better than that of schwertmannite which leads to more electron transfer of MR-1 to Cr(VI). However, schwertmannite has a lower electron transfer efficiency in MR-1+sch+Cr(VI).

### *3.4. Verification of the mechanism of which secondary minerals enhance Cr(VI) removal*

Based on the above results, we deduced that the mechanism of secondary minerals enhance the Cr(VI) removal includes the following three mechanisms: adsorption of Cr(VI), indirect electron transfer by Fe(III)/Fe(II) cycling in minerals, and indirect electron transfer by conduction band electrons.

To further verify the above three promotion mechanisms, hematite was selected for comparative study. Hematite has been reported to indirectly promote electron transfer of MR-1 through Fe(III)/Fe(II) transformation and conduction band electrons directly (Meitl et al., 2009). Meanwhile, electrochemical impedance spectroscopy (EIS) was used to further verify the electron transfer mechanism in MR-1+secondary mineral+Cr(VI) (Fig. S4). Based on previous studies, an equivalent circuit Rs(Q1(R1(R2Q2))) (Fig. 6B) was proposed to fit the experimental impedance data. Rs and R1 correspond to the solution resistance and charge transfer resistance during the oxidation of schwertmannite or jarosite. The fitting results are shown in Table 1.

In this study, similar lactate consumption was observed in MR-1+hem+Cr(VI), MR-1+sch+Cr(VI) and MR-1+jar+Cr(VI) (Fig. 7B). Meanwhile, the removal of Cr(VI) promoted by hematite is the same as that of schwertmannite (Fig. 7A). Nevertheless, the resistance of hematite (4260Ω) is approximately ten times lower than that of schwertmannite (42526Ω) (Table 1), indicating that hematite has a significantly higher direct electron transfer capacity than schwertmannite. The result indicate that the removal capacity of Cr(VI) by schwertmannite is better than that of hematite through adsorption and Fe(III)/Fe(II) cycling. It has been reported that the Fe(III)/Fe(II) transformation is a vital method for hematite to promote electron transfer capacity. Therefore, we speculated that in the removal of Cr(VI), the adsorption of schwertmanniteny may account for a large proportion. In addition, the reduction of Cr(VI) promoted by hematite is lower than that of jarosite. The direct electron transfer of jarosite may play an important role in promoting Cr(VI) bioreduction because the resistance of jarosite is approximately 30 times smaller than that of hematite.

Table 1 shows that the resistance of the original schwertmannite (42526 Ω) is 282.75 times higher than that of the original jarosite (150.4 Ω), which indicates that the direct electron transfer efficiency of jarosite is higher than that of schwertmannite in the early stage of the reaction. Meanwhile, the resistance decreases by 12.48 times compared with the original schwertmannite in the sch/Cr(VI) system, which may be due to the collapse of the structure of schwertmannite, as determined from the SEM and XRD results (Fig. S3), consistent with the conclusion of previous paper (Jia et al.,

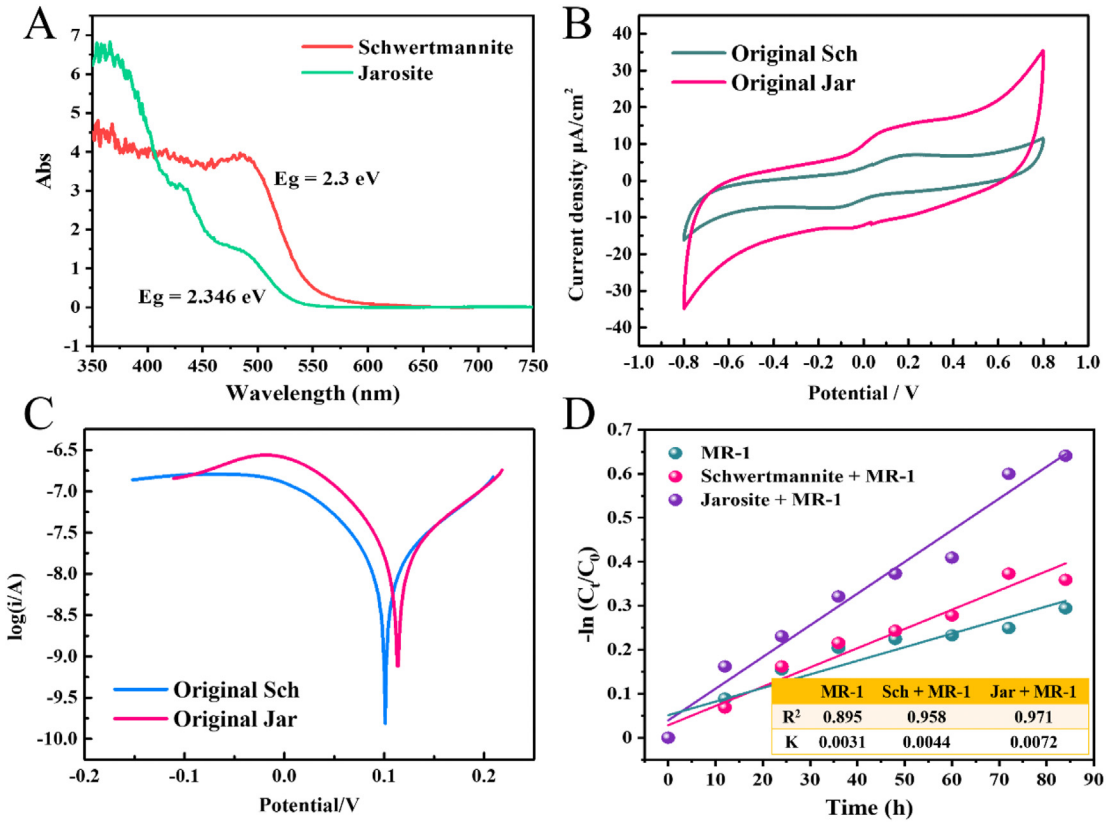


**Fig. 5.** UV–vis diffuse reflection spectra of original schwertmannite and jarosite (A); Cyclic voltammograms (B), Tafel corrosion scan (C) of original schwertmannite and jarosite; The first-order kinetic curve of Cr(VI) bio-reduction (D).

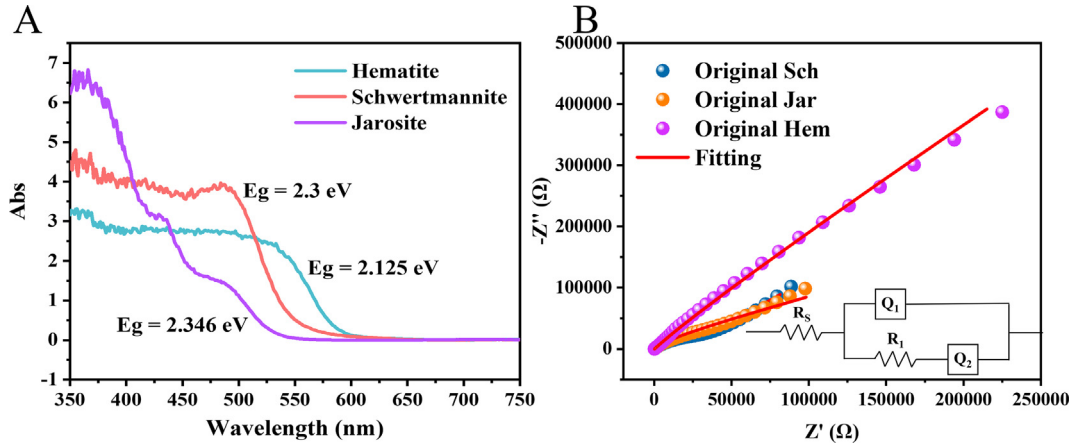


**Fig. 6.** UV–vis diffuse reflection spectra and electrochemical impedance spectroscopy of original schwertmannite, jarosite and hematite(A, B).

**Table 1**
Fitting results of EIS spectra of secondary minerals measured by equivalent circuit Rs(Q1(R1Q2)).

| | Rs/Ω | Q1 | R1/Ω | Q2 |
|---|---|---|---|---|
| Original Sch | 165.8 | 5.0499e-6 | 42526 | 2.0425e-5 |
| Sch + Cr(VI) | 161.7 | 1.7067e-6 | 3408 | 1.0384e-5 |
| Sch + MR-1 + Cr(VI) | 175.6 | 1.7421e-6 | 8303 | 6.3851e-6 |
| Original Jar | 172.9 | 2.5507e-6 | 150.4 | 1.0438e-5 |
| Jar + Cr(VI) | 167.2 | 1.6834e-6 | 4871 | 8.2026e-6 |
| Jar + MR-1 + Cr(VI) | 173.7 | 2.0495e-6 | 5894 | 4.8246e-6 |
| Original Hem | 170.5 | 2.523e-6 | 4260 | 4.4616e-6 |

2012). Therefore, in MR-1+sch+Cr(VI), we deduced that the adsorption of Cr(VI) may enhance the conductivity of schwertmannite, thus enhancing the direct electron transfer efficiency. The resistance of schwertmannite in MR-1+sch+Cr(VI) is lower than that in the sch/Cr(VI) system, which may be due to the attachment of Cr(III) on the surface of schwertmannite, according to XPS data. In contrast, the original jarosite has excellent conductivity because the resistance of the mineral is only 150.4 Ω. Meanwhile, in MR-1+S-mineral+ Cr(VI), the resistance of jarosite (5894 Ω) is still significantly lower than that of schwertmannite (8303 Ω) after the reaction. Thus, in MR-1+S-mineral+ Cr(VI), we speculated that the electron transfer efficiency of jarosite is higher than that of

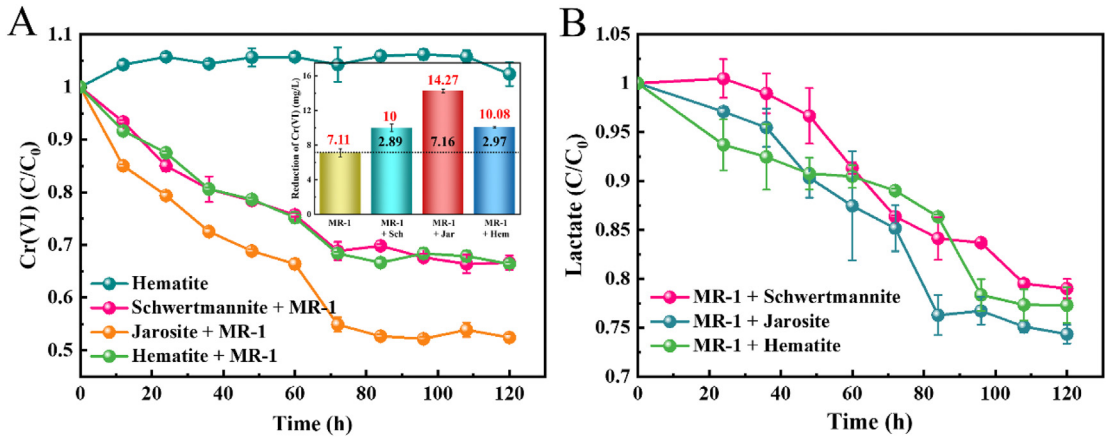


**Fig. 7.** Cr(VI) reduction (a), lactate consumption (b) and comparison of reduction amount of Cr(VI) in different experimental systems.

schwertmannite throughout the reaction periods. Taking all the factors above into consideration, we deduced that the direct electron transfer rate of jarosite is obviously higher than that of schwertmannite, contributing to the reduced Cr(III) amount on jarosite 10 times higher than that on schwertmannite.

### *3.5. Proposed removal pathways of Cr(VI) in MR-1 + secondary minerals + Cr(VI)*

Based on the results herein, we speculated that the Cr(VI) removal pathways in MR-1+secondary minerals+Cr(VI) are (Fig. 8): (i) direct reduction of MR-1, (ii) adsorption of secondary minerals, (iii) indirect reduction of Cr(VI) through Fe(III)/Fe(II) cycling in secondary minerals, and (iv) reduction of Cr(VI) by secondary minerals that directly mediate electron transport. Meanwhile, different secondary minerals have different electron transfer mechanisms. In MR-1+sch+Cr(VI), schwertmannite indirectly mediate electron transfer to Cr(VI) mainly by Fe(III)/Fe(II) cycling in the initial stage (state 1), and hardly transfers electrons directly owing to the high resistance. Under the activation of MR-1 and Cr(VI), the pompon-like structure of schwertmannite shrinks, which decreases the electrical resistance and enhances the direct electron transfer rate of schwertmannite. Thus, we deduced that in the stage 2, schwertmannite directly and indirectly mediated electron transfer. But the direct electron transfer rate of schwertmannite is still lower than that of jarosite because the resistance of schwertmannite is significantly lower than that of jarosite (Table 1). Jarosite with semiconductor properties has low resistance. In MR-1+jar+Cr(VI), jarosite directly promotes the electron transfer which is from MR-1 to Cr(VI) by conduction band electron or Fe(III)/Fe(II) in state 1 and 2.

## 4. Conclusions

Secondary minerals have been demonstrated to interfere with the EET of microorganisms and, thus, the migration and transformation of heavy metals in the subsurface. Combining wet chemistry, spectroscopy, and electrochemical analysis, we found that the mechanisms of secondary minerals as redox mediators enhancing Cr(VI) bioreduction with *shewanella oneidensis* MR-1 included direct conduction band electron transfer, indirect electron transfer through cycling between Fe(III) and Fe(II), and

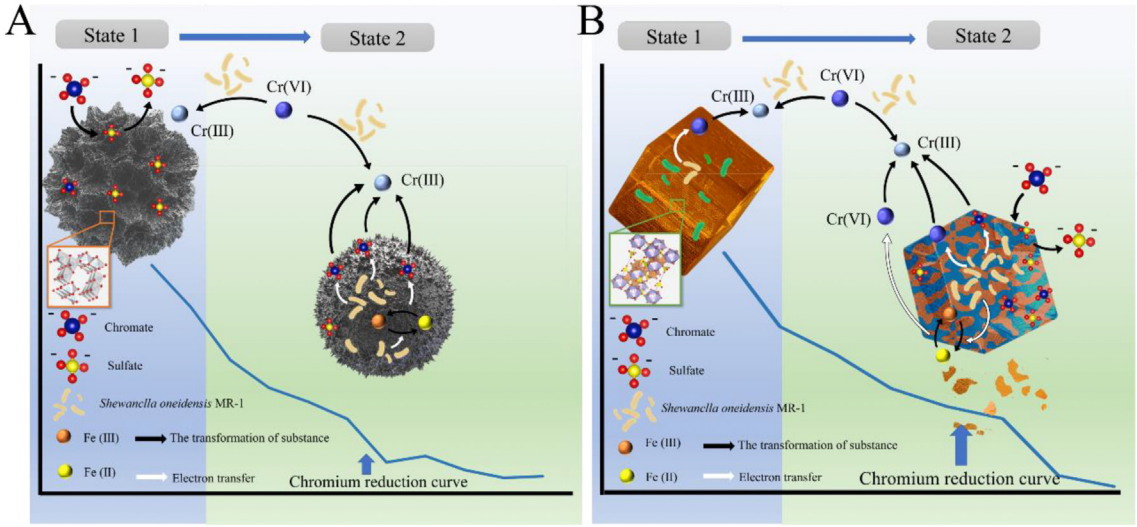


**Fig. 8.** The reduction mechanism of Cr(VI) in MR-1 + schwertmannite + Cr(VI) (A) and in MR-1 + jarosite + Cr(VI) (B).

chromate adsorption through sulfate ligand exchange. Our study provided additional information about different secondary minerals facilitating EET of *shewanella oneidensis* MR-1. Furthermore, this study provides a basic for a better understanding of the interactions between secondary minerals, MR-1, and Cr(VI) or other metals in complex subsurface environments.

## Author statement

Jianyu Zhu: Funding acquisition, Conceptualization, Methodology. Ke Zhang: Data curation, Writing – original draft, Writing-Reviewing and Editing, Funding acquisition. Na Li: Investigation. Peng Liao: Supervision. Yuwen Jin: Investigation. Qiongyao Li: Investigation. Min Gan: Writing- Reviewing and Editing, Funding acquisition. Yaozong Chen: Software. Peng He: Software. Fang Chen: Software. Mingxian Peng: Data curation.

## Declaration of competing interest

The authors declare that they have no known competing financial interests or personal relationships that could have appeared to influence the work reported in this paper.

## Acknowledgements

This work was supported by the National Natural Science Foundation of China (NO. 41773089, 51804350); Natural Science Foundation of Hunan province (2019JJ50769); postdoctoral foundation for MG from Chinese PD science foundation (2017M610506, 2018T110842, 185690); Open Sharing Fund for the Large-scale Instruments and Equipments of Central South University (CSUZC201909); Fundamental Research Funds for the Central Universities of Central South University.

## Appendix A. Supplementary data

Supplementary data to this article can be found online at https://doi.org/10.1016/j.envpol.2021.117227.

## References

Agrawal, A., Kumar, V., Pandey, B.D., 2006. Remediation options for the treatment of electroplating and leather tanning effluent containing chromium - a review. Miner. Process. Extr. Metall. Rev. 27, 99–130.

Aguilar-Carrillo, J., Herrera-Garcia, L., Reyes-Dominguez, I.A., Gutierrez, E.J., 2020. Thallium(I) sequestration by jarosite and birnessite: structural incorporation vs surface adsorption. Environ. Pollut. 257.

Byrne, J.M., Klueglein, N., Pearce, C., Rosso, K.M., Appel, E., Kappler, A., 2015. Redox cycling of Fe(II) and Fe(III) in magnetite by Fe-metabolizing bacteria. Science 347, 1473–1476.

Cheng, Z.-H., Xiong, J.-R., Min, D., Liu, D.-F., Li, W.-W., Jin, F., Yang, M., Yu, H.-Q., 2020. Promoting bidirectional extracellular electron transfer of *Shewanella oneidensis* MR-1 for hexavalent chromium reduction via elevating intracellular cAMP level. Biotechnol. Bioeng. https://doi.org/10.1002/bit.27305.

Costa, M., Klein, CB., 2006. Toxicity and carcinogenicity of chromium compounds in humans 36, 155–163.

Ding, W., Xu, J., Chen, T., Liu, C.-S., Li, J.-J., Wu, F., 2018. Co-oxidation of As(III) and Fe(II) by oxygen through complexation between As(III) and Fe(II)/Fe(III) species. Water Res. 143, 599–607. https://doi.org/10.1016/j.watres.2018.06.072.

Dou, X., Mohan, D., Pittman Jr., C.U., 2013. Arsenate adsorption on three types of granular schwertmannite. Water Res. 47, 2938–2948.

Fu, L., Li, S.-W., Ding, Z.-W., Ding, J., Lu, Y.-Z., Zeng, R.J., 2016. Iron reduction in the DAMO/*Shewanella oneidensis* MR-1 coculture system and the fate of Fe(II). Water Res. 88, 808–815. https://doi.org/10.1016/j.watres.2015.11.011.

Gan, M., Li, J.-Y., Sun, S.-J., Zheng, Z.-H., Cao, Y.-Y., Zhu, J.-Y., Liu, X.-X., Wang, J., Qiu, G.-Z., 2018. The enhanced effect of *Acidithiobacillus ferrooxidans* on pyrite based Cr(VI) reduction. Chem. Eng. J. 341, 27–36. https://doi.org/10.1016/j.cej.2018.02.014.

Gan, M., Sun, S., Zheng, Z., Tang, H., Sheng, J., Zhu, J., Liu, X., 2015. Adsorption of Cr(VI) and Cu(II) by AlPO4 modified biosynthetic Schwertmannite. Appl. Surf. Sci. 356, 986–997.

Gong, Y.-F., Werth, C.J., He, Y.-X., Su, Y.-M., Zhang, Y.-L., Zhou, X.-F., 2018. Intracellular versus extracellular accumulation of Hexavalent chromium reduction products by *Geobacter sulfurreducens* PCA. Environ. Pollut. 240, 485–492. https://doi.org/10.1016/j.envpol.2018.04.046.

Han, J.-C., Chen, G.-J., Qin, L.-P., Mu, Y., 2017. Metal respiratory pathway-independent Cr isotope fractionation during Cr(VI) reduction by shewanella oneidensis MR-1. Environ. Sci. Technol. Lett. 4, 500–504.

Han, R., Li, F., Liu, T., Li, X., Wu, Y., Wang, Y., Chen, D., 2016. Effects of incubation conditions on Cr(VI) reduction by c-type cytochromes in intact shewanella oneidensis MR-1 cells. Front. Microbiol. 7.

Holland, S.L., Avery, S.V.J.M., 2011. Chromate toxicity and the role of sulfur, 3, 1119–1123.

James, Bruce, Quality, R.J.J.o.E., 1994. Hexavalent Chromium Solubility and Reduction in Alkaline Soils Enriched with Chromite Ore Processing Residue.

Jia, H.-F., Stark, J., Zhou, L.-Q., Ling, C., Sekito, T., Markin, Z., 2012. Different catalytic behavior of amorphous and crystalline cobalt tungstate for electrochemical water oxidation. RSC Adv. 2, 10874–10881. https://doi.org/10.1039/C2RA21993J.

Jiang, B., Gong, Y., Gao, J., Sun, T., Liu, Y., Oturan, N., Oturan, M.A., 2019. The reduction of Cr(VI) to Cr(III) mediated by environmentally relevant carboxylic acids: state-of-the-art and perspectives. J. Hazard Mater. 365, 205–226.

Kato, S., Hashimoto, K., Watanabe, K., 2012. Microbial interspecies electron transfer via electric currents through conductive minerals. Proc. Natl. Acad. Sci. U. S. A 109, 10042–10046.

Li, Y., Wang, H., Wu, P., Yu, L., Rehman, S., Wang, J., Yang, S., Zhu, N., 2020. Bioreduction of hexavalent chromium on goethite in the presence of Pseudomonas aeruginosa. Environ. Pollut. 265.

Liu, D.-F., Min, D., Cheng, L., Zhang, F., Li, D.-B., Xiao, X., Sheng, G.-P., Yu, H.-Q., 2017. Anaerobic reduction of 2,6-dinitrotoluene by shewanella oneidensis MR-1: roles of Mtr respiratory pathway and NfnB. Biotechnol. Bioeng. 114, 761–768.

Lu, A., Li, Y., Ding, H., Xu, X., Li, Y., Ren, G., Liang, J., Liu, Y., Hong, H., Chen, N., Chu, S., Liu, F., Wang, H., Ding, C., Wang, C., Lai, Y., Liu, J., Dick, J., Liu, K., Hochella Jr., M.F., 2019a. Photoelectric conversion on Earth's surface via widespread Fe- and Mn-mineral coatings. Proc. Natl. Acad. Sci. U. S. A 116, 9741–9746.

Lu, A., Li, Y., Ding, H., Xu, X., Li, Y., Ren, G., Liang, J., Liu, Y., Hong, H., Chen N J P o t N A o S, 2019b. Photoelectric conversion on Earth's surface via widespread Fe-and Mn-mineral coatings, 116, 9741–9746.

Lu, A., Li, Y., Jin, S., Wang, X., Wu, X.-L., Zeng, C., Ding, H., Hao, R., Lv, M., Wang, C.J.N.C., 2012. Growth of non-phototrophic microorganisms using solar energy through mineral photocatalysis, 3, 1–8.

Marshall, M.J., Plymale, A.E., Kennedy, D.W., Shi, L., Wang, Z.-M., 2008. Hydrogenase- and outer membrane *c*-type cytochrome-facilitated reduction of technetium(VII) by *Shewanella oneidensis* MR-1. Environ. Microbiol. 125–136. https://doi.org/10.1111/j.1462-2920.2007.01438.x.

Meitl, L.A., Eggleston, C.M., Colberg, P.J.S., Khare, N., Reardon, C.L., Shi, L., 2009. Electrochemical interaction of Shewanella oneidensis MR-1 and its outer membrane cytochromes OmcA and MtrC with hematite electrodes. Geochem. Cosmochim. Acta 73, 5292–5307.

Melton, E.D., Swanner, E.D., Behrens, S., Schmidt, C., Kappler, A., 2014. The interplay of microbially mediated and abiotic reactions in the biogeochemical Fe cycle. Nat. Rev. Microbiol. 12, 797–808.

Mohamed, A., Yu, L., Fang, Y., Riahi, Y., Uddin, I., Dai, K., Huang, Q.-Y., 2020. Iron mineral-humic acid complex enhanced Cr(VI) reduction by *Shewanella oneidensis* MR-1. Chemosphere 247. https://doi.org/10.1016/j.chemosphere.2020.125902.

Qiu, H., Xu, H., Xu, Z., Xia, B., Peijnenburg, W.J.G.M., Cao, X., Du, H., Zhao, L., Qiu, R., He, E., 2020. The shuttling effects and associated mechanisms of different types of iron oxide nanoparticles for Cu(II) reduction by Geobacter sulfurreducens. J. Hazard Mater. 393.

Rager, J.E., Suh, M., Chappell, G.A., Thompson, C.M., Proctor, D.M., 2019. Review of transcriptomic responses to hexavalent chromium exposure in lung cells supports a role of epigenetic mediators in carcinogenesis. Toxicol. Lett. 305, 40–50.

Regenspurg, S., Peiffer, S., 2005. Arsenate and chromate incorporation in schwertmannite. Appl. Geochem. 20, 1226–1239.

Sheng, L., Fein, J.B., 2014. Uranium reduction by *Shewanella oneidensis* MR-1 as a function of $NaHCO_3$ concentration: Surface complexation control of reduction kinetics. Environ. Sci. Technol. 48 (7), 3768–3775. https://doi.org/10.1021/es5003692.

Shi, L., Dong, H., Reguera, G., Beyenal, H., Lu, A., Liu, J., Yu, H.Q., Fredrickson J K J N R M, 2016. Extracellular Electron Transfer Mechanisms between Microorganisms and Minerals.

Wan, J., Guo, C., Tu, Z., Zeng, Y., Fan, C., Lu, G., Dang, Z., 2018. Microbial reduction of

Cr (VI)-loaded schwertmannite by shewanella oneidensis MR-1. Geomicrobiol. J. 35, 727–734.
Wang, G.-Y., Zhang, B.-G., Li, S., Yang, M., Yin, C.-C., 2017. Simultaneous microbial reduction of vanadium (V) and chromium (VI) by *Shewanella loihica* PV-4. Bioresour. Technol. 227, 353–358. https://doi.org/10.1016/j.biortech.2016.12.070.
Yang, B.-J., Zhao, C.-X., Luo, W., Liao, R., Gan, M., Wang, J., Liu, X.-D., Qiu, G.-Z., 2020. Catalytic effect of silver on copper release from chalcopyrite mediated by *Acidithiobacillus ferrooxidans*. J. Hazard. Mater. 392 https://doi.org/10.1016/j.jhazmat.2020.122290.
Zhang, Z., Guo, G., Li, X., Zhao, Q., Bi, X., Wu, K., Chen, H., 2019. Effects of hydrogen-peroxide supply rate on schwertmannite microstructure and chromium (VI) adsorption performance. J. Hazard. Mater. 367, 520–528.
Zhanna, Sobol, Robert, H., Environmental, S.J., Mutagenesis, M., 2011. Intracellular and Extracellular Factors Influencing Cr(VI and Cr(III) Genotoxicity.
Zhao, Z., Zhang, G., Zhang, Y., Dou, M., Li, Y.J.W.R., 2020. Fe3O4 accelerates tetracycline degradation during anaerobic digestion: synergistic role of adsorption and microbial metabolism, 185, 116225.
Zhi, Shi, John, M., Zachara, Liang, Shi, Zheming, Wang, Science, D.J.E., Technology, 2012. Redox Reactions of Reduced Flavin Mononucleotide (FMN), Riboflavin (RBF), and Anthraquinone-2,6-Disulfonate (AQDS) with Ferrihydrite and Lepidocrocite.